



## **Tutorial: designing solenoid lenses for electron beams**

Stanley Humphries, Copyright 2012

### **Field Precision**

PO Box 13595, Albuquerque, NM 87192 U.S.A.

Telephone: +1-505-220-3975

Fax: +1-617-752-9077

E mail: [techinfo@fieldp.com](mailto:techinfo@fieldp.com)

Internet: <http://www.fieldp.com>

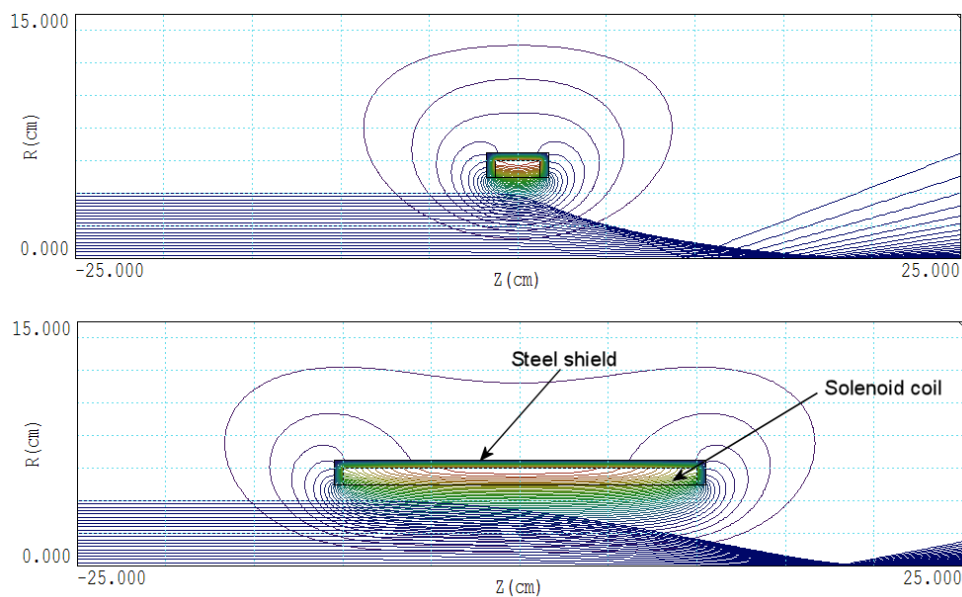


Figure 1: Lines of magnetic flux density and electron orbits,  $f_0/R = 4.0$  a)  $L/R = 0.5$ . b)  $L/R = 4.0$

The solenoid lens is the most common device for focusing and transporting electron beams. Figure 1 shows an  $r$ - $z$  plot of the geometry. The solenoid coil has average radius  $R$  and axial length  $L$ . The magnetic steel shield serves two purposes:

- Limit fringing flux to minimize inference with other optical components or nearby instruments.
- Reduce the number of ampere-turns (and hence the power input) for a given focal length.

In contrast to quadrupole lenses (which must be used in focus-defocus pairs), the solenoid lens provides simultaneous focusing in the  $x$  and  $y$  directions. As a result, solenoids are useful for high-current beam transport or achieving a short focal distance. Section 6.7 of my book **Principles of Charged Particle Acceleration** covers the theory of the solenoid lens and gives analytic approximations for the focal length. The book is available at:

<http://www.fieldp.com/cpa.html>

The usual procedure is to estimate lens characteristics and then turn to a numerical code like **Trak** for a final design.

It is useful to have general rules to guide the choice of  $R$  and  $L$ . The main area of concern is focal quality. Solenoid lenses are subject to spherical

aberration. A lens that produces a radial deflection linearly proportional to the radius of the incident electron orbit produces a perfect focus. In a solenoid lens, the deflection is of the form

$$\Delta r' \sim (r + \alpha r^3) \quad (1)$$

Peripheral particles are over-focused. There is no cylindrically-symmetric defocusing device that can compensate for this effect. For a tight focus, the only option is to limit the beam radius or to reduce  $\alpha$ .

Finding a lens with the desired focal properties by trial-and-error is time-consuming and inefficient. In writing this report, I had two goals:

- Generate numerical lens simulations that illustrate spherical aberration.
- Demonstrate how a scaling analysis makes it possible to infer the behavior of a wide range of systems from a limited set of numerical calculations.

To minimize parameters, I concentrated on radially thin coils where the thickness  $\Delta R$  is small compared to  $R$ . In particular, I used a coil with inner radius  $R = 5.0$  cm and  $\Delta R = 0.5$  cm. Using  $R$  as the primary scaling factor, there is only one free parameter for the coil geometry,  $L/R$ . If the steel shield has  $\mu_r \gg 1$  and regions are not saturated, the shield thickness has little effect on the field distribution. For the calculations, I used a thickness of 0.5 cm.

Specific values of magnetic field magnitude and electron kinetic energy are not critical. The important value is the paraxial lens focal length relative to the coil radius,  $f_0/R$ . The quantity  $f_0$  is the focal point for electrons close to the axis. Here, the  $r^3$  term in Eq. 1 is negligible. In the **Trak** calculations, I investigated two values: a short focus  $f_0/R = 2.0$  and a long focus  $f_0/R = 4.0$ . For the calculations, I created a set of twenty 100 keV electrons that moved parallel to the axis upstream from the lens. The electrons were uniformly distributed in radius to a maximum of 4.0 cm ( $r/R = 0.8$ ). For each lens geometry, I adjusted the coil drive current to achieve the desired paraxial focal point.

For the long focus ( $f_0 = 20.0$  cm relative to the lens midplane), I set up models with coil lengths of  $L = 0.5R$ ,  $L = 1.0R$ ,  $L = 2.0R$  and  $L = 4.0R$ . The drive currents to achieve the focus were 1560.0, 1575.0, 1730.0 and 2170.0 A-turn respectively. For a given radius and focal length, a short coil requires less drive current. On the other hand, the short coil has a significant disadvantage with respect to spherical aberration, as shown in Fig. 1. Forces in the short coil are highly non-linear, resulting in substantial over-focusing of peripheral rays. For the short focus ( $f_0 = 10.0$  cm) I made

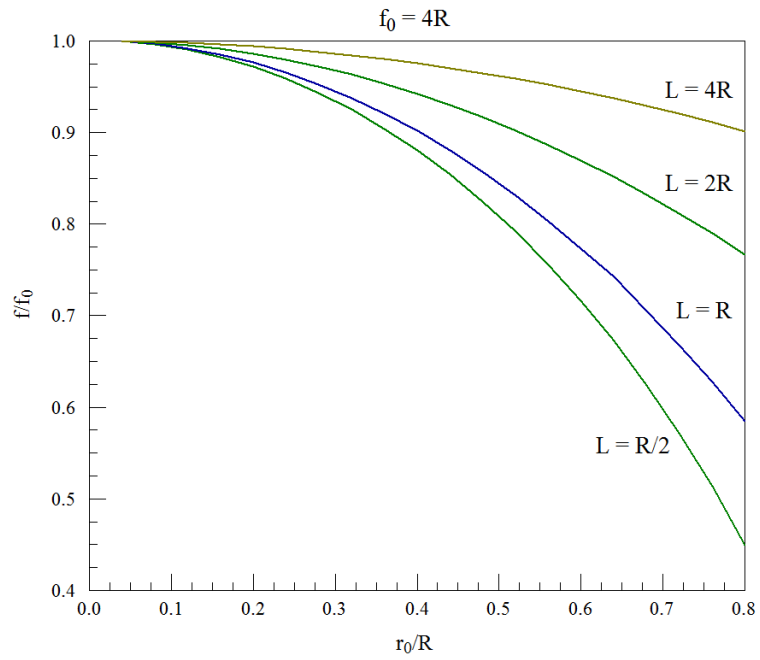


Figure 2: Relative focal length  $f/f_0$  as a function of normalized incident radius  $r_0/R$  for different coil lengths. Short focus:  $f_0 = 2R$ .

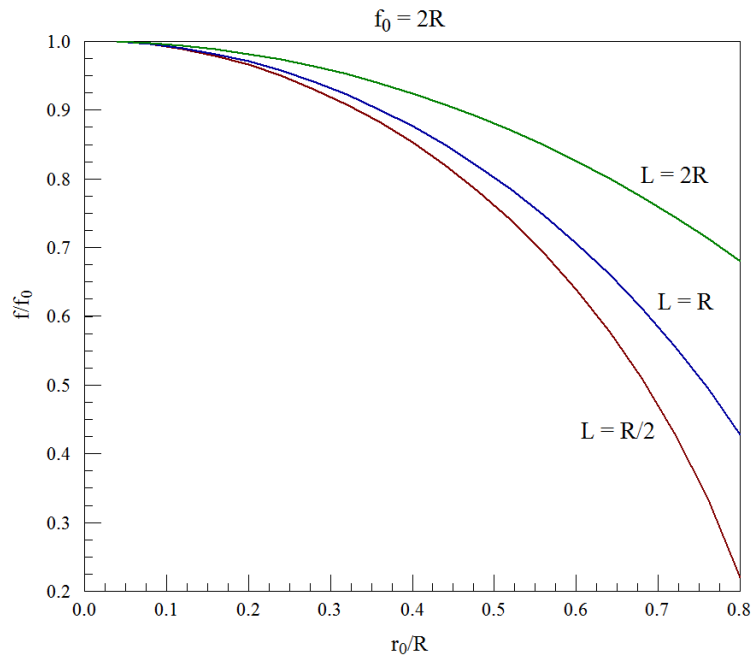


Figure 3: Relative focal length  $f/f_0$  as a function of normalized incident radius  $r_0/R$  for different coil lengths. Long focus:  $f_0 = 4R$ .

calculations for coil lengths of  $L = 0.5R$ ,  $L = 1.0R$  and  $L = 2.0R$ . The associated coil drive currents were 2260.0, 2300.0 and 2540.0 A-turn.

Figures 2 and 3 show the results displayed to emphasize their generality. After adjusting the coil current to set the paraxial focal point  $f_0$ , I determined the effective focal length for outer particles using values of radial and axial momenta in the exit space ( $p_{rf}$  and  $p_{zf}$ ) determined by **Trak** orbit integrals. If  $r_0$  is the particle radius in the entrance space, then the focal length is given by

$$f = \frac{r_0}{\tan(p_{rf}/p_{zf})}. \quad (2)$$

The figures show the relative focal length ( $f/f_0$ ) as a function of the relative entrance radius  $r_0/R$ . As expected from Eq. 1, the deviation in focal length is proportional to  $(r_0/R)^2$ . The figures show that short lenses are considerably worse than longer lenses. The general rule is to make the lens as long as possible consistent with the required focal length. The results are also listed in Tables 1 and 2.

To illustrate application of the data, suppose we want to focus electrons to a point 40 cm from the midplane of a solenoid lens. The lens has bore radius 10.0 cm and length 20.0 cm ( $L/R = 2.0$ ). The beam entering the lens has envelope radius 4.0 cm ( $r_0/R \leq 0.25$ ). From Table 1, the focal length for envelope electrons is  $f/f_0 = 0.942$ . The radius of envelope electrons at the paraxial focal point is

$$r \cong r_0 \frac{f_0 - f}{f_0}. \quad (3)$$

Inserting values, the minimum focal spot radius is about 2.3 mm.

Table 1: Relative focal length as a function of normalized entrance radius for  $f = 4R$ .

$r_i/R$	$f/f_0$ $L = 0.5R$	$f/f_0$ $L = 1.0R$	$f/f_0$ $L = 2.0R$	$f/f_0$ $L = 4.0R$
0.040000	1.000000	1.000000	1.000000	1.000000
0.080000	0.996437	0.996968	0.998200	0.999212
0.120000	0.990493	0.992036	0.995324	0.998007
0.160000	0.982279	0.985169	0.991234	0.996307
0.200000	0.971638	0.976354	0.986012	0.994098
0.240000	0.958595	0.965500	0.979630	0.991415
0.280000	0.943075	0.952675	0.972058	0.988231
0.320000	0.924906	0.937740	0.963349	0.984569
0.360000	0.904076	0.920737	0.953446	0.980401
0.400000	0.880531	0.901636	0.942392	0.975735
0.440000	0.854030	0.880377	0.930163	0.970600
0.480000	0.824577	0.856939	0.916755	0.964941
0.520000	0.791833	0.831248	0.902183	0.958794
0.560000	0.755818	0.803322	0.886426	0.952139
0.600000	0.715950	0.773042	0.869458	0.944966
0.640000	0.672111	0.745303	0.851336	0.937251
0.680000	0.624105	0.705295	0.832044	0.929061
0.720000	0.571557	0.667788	0.811555	0.920277
0.760000	0.513434	0.627724	0.789822	0.910968
0.800000	0.449452	0.585201	0.766858	0.901036

Table 2: Relative focal length as a function of normalized entrance radius for  $f = 2R$ .

$r_i/R$	$f/f_0$ $L = 0.5R$	$f/f_0$ $L = 1.0R$	$f/f_0$ $L = 2.0R$
0.040000	1.000000	1.000000	1.000000
0.080000	0.995749	0.996387	0.997789
0.120000	0.988667	0.990301	0.993968
0.160000	0.978701	0.981777	0.988689
0.200000	0.965801	0.970796	0.981879
0.240000	0.949845	0.957272	0.973536
0.280000	0.930732	0.941170	0.963650
0.320000	0.908318	0.922420	0.952252
0.360000	0.882601	0.900826	0.939199
0.400000	0.853165	0.876502	0.924517
0.440000	0.819773	0.849167	0.908204
0.480000	0.782109	0.818736	0.890305
0.520000	0.739921	0.784983	0.870593
0.560000	0.692445	0.747658	0.849216
0.600000	0.639012	0.706600	0.825992
0.640000	0.578644	0.661389	0.800896
0.680000	0.509892	0.611552	0.773950
0.720000	0.430544	0.556610	0.744958
0.760000	0.336129	0.495636	0.713929
0.800000	0.219426	0.427363	0.680709